Second Harmonic Spectroscopy of Aqueous Nano- and Microparticle Interfaces

Kenneth B. Eisenthal

Department of Chemistry, Columbia University, New York, New York 10027

Received May 13, 2005

Contents

1. Introduction

Applications of the interface-selective methods of second harmonic (SHG) and sum frequency (SFG) spectroscopy to the investigation of equilibrium and time-dependent properties of interfaces are increasing at an explosive rate.[1−53] Among the interfaces studied with these methods are liquid/gas, solid/gas, and the buried liquid/liquid, liquid/solid, and solid/solid interfaces.[35,36,39,41,51,53] In 1996, I was able to write a *Chemical Reviews* article that was a reasonably comprehensive review of the field. However today, this would require a book-length review if only second harmonic spectroscopy was considered. Though restricting the review to aqueous interfaces for the purposes of this *Chemical Reviews* issue is helpful, it does not reduce the extensive research topics to a manageable length. On the basis of these considerations, I have limited the review to a rapidly growing area of research, which uses SHG as the primary method. This new area addresses the aqueous interfaces of nano- and microsize particles suspended in aqueous solutions. These small particles in aqueous solution are commonly referred to as colloids. Although colloidal chemistry is a well-established field, important in basic science, technology, and medicine,[54,55] it is only in the past decade that SHG and SFG spectroscopies have been used specifically to probe aqueous colloid surfaces. One can anticipate that SHG and SFG will have a major impact on the future development of interfacial colloid chemistry.

Kenneth B. Eisenthal received a B.S. in chemistry from Brooklyn College and an M.A. in physics and a Ph.D. in chemical physics from Harvard University. He did postdoctoral research at UCLA and was at IBM Almaden Research Division Laboratory before coming to Columbia University in 1975.

2. Second Harmonic Generation and Centrosymmetry

The origin of the interface specificity of these second-order nonlinear spectroscopies is the intrinsically noncentrosymmetric structure of interfaces. It is commonly assumed that SHG and SFG are forbidden in centrosymmetric systems but not at the noncentrosymmetric interface.[56,57] A consequence of this viewpoint is that most SHG and SFG studies have been carried out on noncentrosymmetric planar surfaces

10.1021/cr0403685 CCC: $59.00
Published on Web 03/30/2006

that separate centrosymmetric and isotropic bulk media, for example, bulk liquids and amorphous and centrosymmetric solids. The bulk centrosymmetric systems do not radiate coherent SHG because of symmetry reasons. The symmetry argument is that for every molecule oriented in one direction, there is a neighboring one oriented in the opposite direction. The nonlinear polarizations induced in these oppositely oriented molecules by the incident light are of opposite phase with respect to each other and thus cancel. Therefore the net second-order polarization is zero, and there is no coherent SHG or SFG radiated from the bulk. If it was otherwise, the bulk signal would overwhelm the interface signal because of the much greater amount of material in the bulk than at the interface. Although coherent SHG and SFG is not generated in bulk centrosymmetric media owing to the cancellation discussed above, the fluctuations in molecular density and molecular orientation in isotropic bulk solutions can disrupt the phase cancellation. In this way, incoherent second-order light scattering, called hyper-Rayleigh scattering, is generated and has been observed in bulk centrosymmetric media.[58,59] SHG can also be generated by individual large noncentrosymmetric entities in bulk solution, as has been observed in randomly oriented suspensions in solution.[60] The origin of the SHG signal in this case was chiefly the noncentrosymmetric interior region of the individual microscopic particles. Semiconductor quantum dots and metallic crystals also give rise to SHG, which has also been attributed to their noncentrosymmetric structure.[61]

2.1. Theoretical Considerations

At this point, we want to look more closely at the relationship between the symmetry of the system and the generation of light at 2ω and at the sum frequency $\omega_1 + \omega_2$ of the incident light fields. Although SHG and SFG are commonly asserted to be forbidden in centrosymmetric systems, this is true only if the system is centrosymmetric on length scales much less than the coherence length of the process.

To establish this central idea, let us consider a system consisting of two sheets, each of which is noncentrosymmetric, that together form a centrosymmetric structure as shown in Scheme 1. The sheets, which are separated by a

Scheme 1

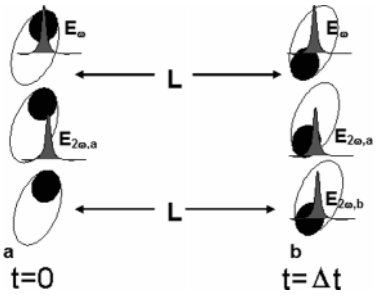

distance L, have a centrosymmetric homogeneous substance in the space between them, which is characterized by a refractive index $n(\omega)$ at the frequency ω and a refractive index $n(2\omega)$ at the frequency 2ω. The reason that this centrosymmetric system is chosen to illustrate the underlying idea, rather than a centrosymmetric sphere, for example, is that the nonlinear polarization, $P^{(2)}_{(2\omega)}$, induced in a sheet by the incident light field is the same at all positions in the sheet. This applies to both sheets.

Referring to the centrosymmetric structure in Scheme 1, we note that the second harmonic (or sum frequency) electric field, $E_a(2\omega)$, generated at sheet a propagates across the separation L to the position of sheet b. The fundamental light at ω, which is not depleted, propagates to sheet b where it generates radiation at 2ω of amplitude $E_b(2\omega)$ equal in magnitude to $E_a(2\omega)$. The resultant second harmonic electric field $E(2\omega)$ is the sum of the fields $E_a(2\omega)$ and $E_b(2\omega)$. The magnitude of the total electric field, $E(2\omega)$, depends on the relative phase of the two fields, that is, it is the phase that determines whether there is constructive or destructive interference. Because the incident field at ω propagates across the distance L with a different phase velocity than the second harmonic $E_a(2\omega)$ generated at a, there is a phase shift of $E_a(2\omega)$ with respect to $E_b(2\omega)$. The difference in the phase of $E_a(2\omega)$ and $E_b(2\omega)$ is

$$\delta = (k_{2\omega} - 2k_{\omega})L = \frac{2\omega}{c}[n(2\omega) - n(\omega)]L \qquad (1)$$

The sum of the two fields is $E_a(2\omega) + E_b(2\omega) \propto E_o(2\omega)[e^{i\delta} - 1]$, where $E_o(2\omega)$ is the magnitude of the second harmonic field generated from each sheet.

For $L \ll \lambda$, as is the case for a bulk isotropic solvent where the molecules are separated by angstroms, for example, water, the phase difference δ is essentially zero. Thus the sum of the second harmonic fields is zero as is expected for an isotropic system, and no coherent SH is generated. If, however, δ is not zero for a given L, it follows that a strong coherent second harmonic signal can be generated. Note that if $\delta = \pi$, the total radiated field is twice that of each sheet, and the intensity is four times that of an individual sheet. We conclude therefore that SHG is allowed and can be strong for centrosymmetric structures whose dimensions are determined by eq 1, typically on the order of the wavelength or some fraction of the wavelength of the SHG light. As the dimension L of the centrosymmetric particle decreases, destructive interference increases, that is, there is increasing cancellation and the SHG signal decreases. At wavelengths $\lambda \gg L$, a centrosymmetric object will still generate a SHG signal, but now there is increased cancellation of the second-order polarization from the various locations in the particle.

2.2. Demonstration Experiments of SHG from Centrosymmetric Particles

The initial experiments, which demonstrated that centrosymmetric structures can generate coherent SH signals, used 1 μm polystyrene sulfate (PSS) microspheres suspended in an aqueous solution containing the cationic triphenylmethane dye malachite green (MG)[62] (Scheme 2).

Scheme 2. Malachite Green (MG)

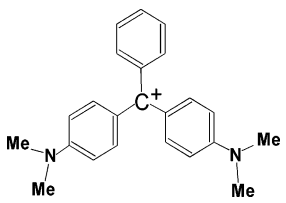

The experiments showed that the strong SHG signal was due to MG adsorbed to the microsphere surface and not to MG free in the solution nor to the microspheres without MG. Parenthetically, MG has become a popular molecule in interfacial studies because of its large hyperpolarizability,

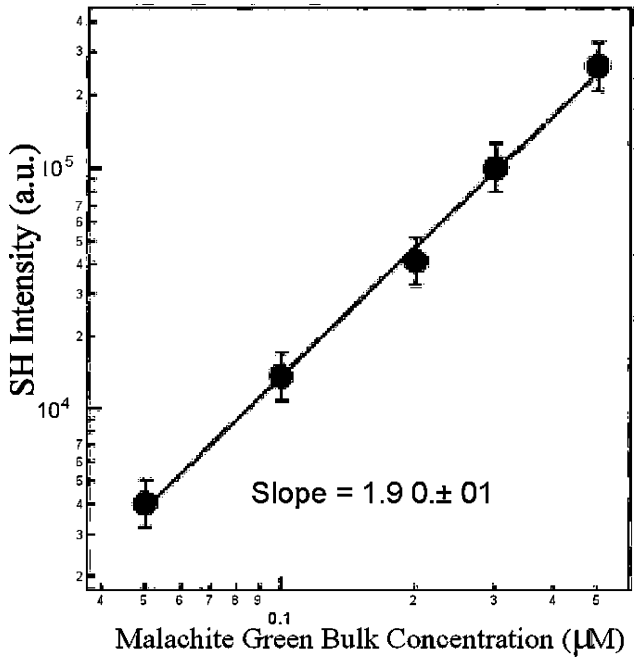

Figure 1. Second harmonic signal as a function of bulk MG concentration at a density of 8.3×10^8 polystyrene sulfate microspheres/cm^3 at low MG concentrations. Reprinted with permission from ref 62. Copyright 1996 Elsevier.

which is resonantly enhanced at twice the frequency of the output of commonly used Ti:sapphire femtosecond lasers. It was found, as expected for a second-order optical process, that the SH signal scaled quadratically with the incident light intensity, $I(\omega)$.[62] To determine whether the SHG from the individual spheres is coherently generated, it is necessary to investigate how the SHG signal, $I_{2\omega}^{\text{total}}$, varies with the density of adsorbates. If the SH signal originating from each of the spheres is coherently generated, $I_{2\omega}^{\text{total}}$ should scale quadratically with the density of MG adsorbed on the PSS surface.

The total SH signal is given by

$$I_{2\omega}^{\text{total}} \propto |\sum_{j=1}^{n} E_j^{2\omega}\, e^{i\phi_j}|^2 = \sum_{j=1}^{n}\sum_{k=1}^{n} E_j^{2\omega}\, E_k^{2\omega}\, e^{i(\phi_j-\phi_k)} \qquad (2)$$

where $E_j^{2\omega}$ is the second harmonic electric field generated by the jth PSS microsphere and ϕ_j is the phase of the second harmonic electric field generated by sphere j. For a low density n of microspheres, the SHG from each microsphere is independent of other spheres, and their phases are random. Thus only the $j = k$ terms survive, giving

$$I_{2\omega}^{\text{total}} \propto \sum_{j=1}^{n} (E_j^{2\omega})^2 = n(E^{2\omega})^2 = nI_{2\omega} \qquad (3)$$

where $I_{2\omega}$ is the SHG from a single sphere. Figure 1 shows that $I_{2\omega}^{\text{total}}$ scales quadratically with the MG concentration, which means that $I_{2\omega}$, the SHG from an individual sphere, is generated coherently.[62]

We see from eq 3 that $I_{2\omega}^{\text{total}}$, which is the total SHG signal, scales linearly with the number of spheres, characteristic of an incoherent summation, and is called hyper-Rayleigh scattering. The experimental results[62] showed the linear dependence on the density of PSS microspheres in accord with an incoherent process. If the density of particles was sufficiently high such that the particle−particle distance was less then the coherence length, then the phases of the second harmonic electric field of the particles would not be random and the summation over all particles would not yield a linear dependence on particle density. From this brief discussion, we see that information about the microsphere/aqueous interface, which is our objective, is contained in the coherent second harmonic scattering from the individual microsphere/aqueous interface.

The discussion up to this point has focused on SHG of centrosymmetric structures. As noted earlier strong SFG signals can also be generated by centrosymmetric nanoparticles and microparticles. This was shown to be the case with the generation of 278 nm light when laser pulses at 834 and 417 nm irradiated an aqueous solution containing MG molecules adsorbed to the surfaces of the PSS microspheres.[63,64] We conclude that both SHG and SFG can selectively probe the interfaces of centrosymmetric microparticles.

A few remarks at this point about some general experimental conditions could be helpful to the reader. In carrying out the SHG experiments, it is necessary to separate the SHG signal at 2ω from other optical signals such as linear (Rayleigh) scattering of the strong fundamental at ω, hyper-Raman scattering, and fluorescence. To effect this separation, appropriate filters plus a monochromator are required. In most of the experiments, ultrashort light pulses, mostly of femtosecond duration but also of picosecond duration, are used because the SHG signal is quadratically dependent on the intensity of the incident light. Thus if the pulse duration is decreased by a factor of 10, the SHG signal is increased by a factor of 100. The value of higher powers increases until the breakdown of the sample occurs due to multiphoton ionization and dissociation of the chemical species present in the solution. Thus the maximum laser power that is below the threshold for breakdown will yield the optimum SHG signal.

2.3. Free Energy of Adsorption

The energetics that drive molecules from the bulk of a solution to an interface provide information on the molecule's interactions with the chemical species in the bulk liquid and in the interfacial regions. Interactions such as solvation, hydrophobicity, and hydrogen bonding can be markedly different in the bulk and interface regions.[54,55] Knowledge of the populations of chemical species adsorbed to a microparticle/aqueous interface and the energetics of adsorption are needed in the description of any aqueous interface. The traditional technique used to obtain adsorbate density populations at solid microparticle/aqueous interfaces is the centrifugation−separation method.[65−75] The procedure is to measure, using absorption spectroscopy, the concentration of the solute molecules of interest in solution with no microparticles present. After addition of the microparticles, the solution is centrifuged, and the concentration in the supernatant is measured. The difference in the absorption with and without the microparticles is equal to the concentration of solute molecules that have been adsorbed to the particle/aqueous interfaces. By repetition of these measurements on solutions at different solute concentrations, a way is provided to determine the free energy of adsorption. This method has proven to be simple and useful; however there are a number of difficulties. One is the assumption that on centrifugation the molecules of interest that were in solution

are not trapped in the residue after centrifugation. Another factor is the possible change in the microparticle interfaces, which can affect the adsorbate population, as the separations between the particles are greatly reduced on centrifugation.

With the SHG method, we have a new and noninvasive way to obtain the free energy of adsorption and the density of adsorbates as a function of bulk concentration.[63] The quantitative relationship of the adsorbate population with its bulk concentration is given by the adsorption isotherm. A reasonably good description of the equilibrium between molecules in the liquid and those that are adsorbed to the interface is provided by the Langmuir model.[54,55] In this model, which is usually applied to planar interfaces, the adsorption of the bulk molecules M is treated as the filling of empty surface sites (ES), assumed to be noninteracting, by the bulk molecules M and the reverse process in which a filled site (FS) is emptied with the adsorbate going into the bulk phase. This can be expressed as

$$\mathrm{M} + \mathrm{ES} \underset{k_{-1}}{\overset{k_1}{\rightleftharpoons}} \mathrm{FS} \tag{4}$$

The equilibrium constant K and its relation to the free energy of adsorption $\Delta G°$ is

$$K = \mathrm{e}^{-\Delta G°/(RT)} = \frac{k_1}{k_{-1}} = \frac{[\mathrm{FS}]}{[\mathrm{M}][\mathrm{ES}]} \tag{5}$$

In the Langmuir model, the depletion of molecules in the bulk phase is neglected because planar surfaces, even at saturation, have a population that is almost always negligible compared with the bulk population. This may not be a valid assumption for microparticles in solution because the total surface area can be very large. A modified Langmuir model[63] that includes the depletion of molecules M in the bulk solution yields the following expression:

$$\frac{N}{N_{\max}} = \frac{(C + N_{\max} + 55.5/K) - \sqrt{(C + N_{\max} + 55.5/K)^2 - 4CN_{\max}}}{2N_{\max}} \tag{6}$$

where N is the number of moles of adsorbed molecules per liter, $N_{\max}$ is the maximum concentration that can be adsorbed, C is the bulk concentration of M and 55.5 is the molarity of water. The second harmonic electric field is proportional to the adsorbate density N. From a fitting of eq 6 to SHG measurements[63] on an aqueous solution containing 1 μm polystyrene particles (10^8/cm^3) and MG both (see Figure 2),the maximum number of adsorbed MG per PSS particle was found to be $(1.8 \pm 0.2) \times 10^6$, and the adsorption free energy, which is the driving force for the adsorption, was found to be $\Delta G° = -11.1 \pm 0.1$ kcal/mol.

2.4. Detection of Adsorbates Having Small Hyperpolarizabilities

There are important technologies that employ surfactant coating of emulsions and colloids to achieve desired properties, for example, dispersion stability, size and color, textile processing, pharmaceutical preparations, paints, oil drilling, and pesticides, to name just a few.[66−75] For many of these applications, it has been found that the surfactants have small hyperpolarizabilities.[76] Information on surfactant populations and adsorption free energies for microparticle emulsions and colloids is of great value in science, technology, and medicine.[54,55,77] Traditional methods have important limitations, as does the SHG method for species with small hyperpolarizabilities.[66−76] Because of this limitation, it is virtually impossible to detect their adsorption onto microparticle surfaces using SHG. One novel way to circumvent this detection problem is to measure the reduction of a strong SHG signal due to dye molecules adsorbed to the microparticle interface as the dye is displaced by a methacrylate-based surfactant.[76] Experiments designed to test this approach employed an aqueous solution containing 1 μm PSS microspheres and our old friend MG, a commonly used dye, as the molecule to be displaced by the surfactant. This method works and has been successfully applied to surfactant adsorption and biopolymer poly(L-lysine) adsorption onto polystyrene microspheres[76,78] (Figure 3). The dye displacement method has also been successfully applied to the displacement of bromocresol purple by surfactants adsorbed to the surfaces of talc microparticles (mica-like structures) suspended in an aqueous solution.[76]

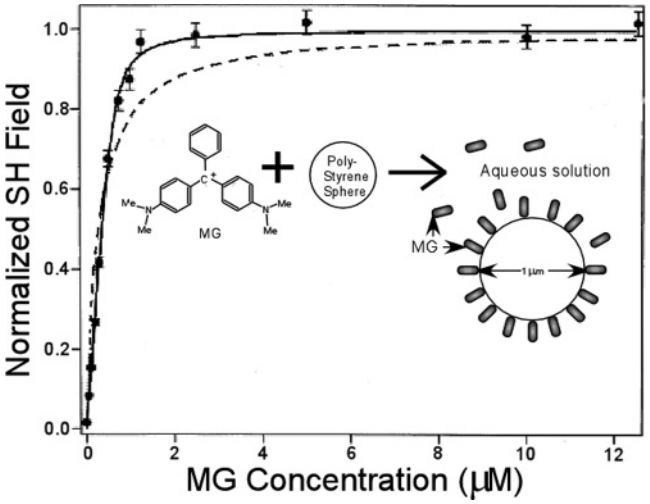

Figure 2. Adsorption isotherm of Malachite Green (MG) and polystyrene sulfate (PSS) microspheres. A fit with the Langmuir model (dashed line) gives $\Delta G° = -10.5 \pm 0.1$ kcal/mol, while a fit with the modified Langmuir model (solid line) gives $\Delta G° = -11.1 \pm 0.1$ kcal/mol.

2.5. Electrostatics of Adsorption

The effects of surface charge density on the properties of nano- and microparticle/aqueous interfaces are considerable. For example, at the interface of a negatively charged surface, the pH will be lowered significantly compared with the bulk pH, and with similar considerations interfaces have a higher pH at a positively charged surface compared with the bulk pH. Of course, these electrostatic effects apply to all charged species and to the orientation and populations of charged and polar molecules in the region of the interface. A recent study[79] of the aqueous interfaces of 1 μm polystyrene microspheres that were negatively charged (PSS), positively charged (PSA), and essentially neutral (PS) has shed new light on this question. The MG adsorption free energies for the negatively charged PSS, the neutral PS, and the positively charged PSA were found to be −12.67, −12.30, and −10.46 kcal/mol, respectively. The result that the free energy for the negatively charged PSS, which has a strong electrostatic

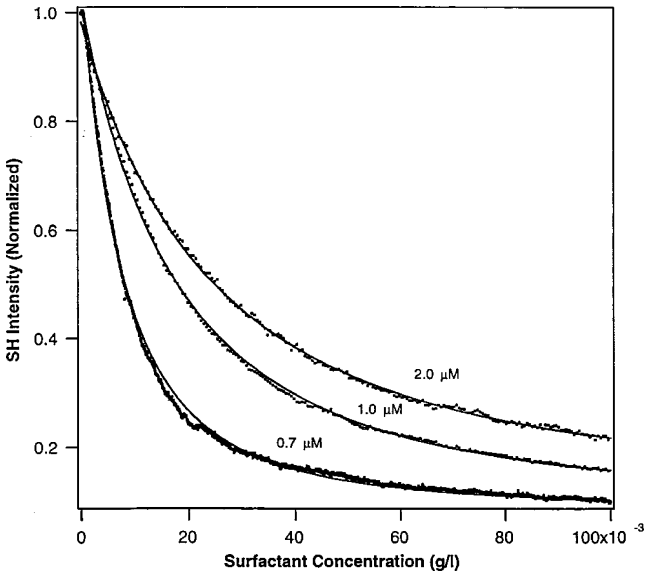

Figure 3. Reduction in SH intensity due to MG dye displacement by a methacrylate-based surfactant. The MG concentrations in the aqueous solution are marked near the curves. The points are experimental data. The solid lines are theoretical fits. Reprinted with permission from ref 76. Copyright 2000 American Chemical Society.

interaction with the cationic dye MG, is only slightly more negative than the neutral PS is surprising. It indicates that there are significant non-Coulombic interactions between MG and the various polystyrene microspheres. The contributions of van der Waals forces, hydrophobic forces between polystyrene and MG, hydrogen bonding, and the effects of water solvation of the negative sulfate moiety of PSS and the weak solvation of MG must be considered in reconciling the small ΔG differences. The observation that MG adsorbs to positively charged PSA microspheres, though much more weakly than the others, further indicates the importance of these non-Coulombic forces. Electrophoresis measurements to determine the actual charges of the PSS and PSA microspheres would be helpful. It would also be useful to determine whether there is any residual charge on the neutral PS following the styrene polymerization.

2.6. Adsorption to Liquid Microparticle/Aqueous Interface

Another microparticle/aqueous interface of considerable interest in medicine and technology is the oil droplet/aqueous interface of an oil−water emulsion.[54,55,77] Measurement of the adsorption of molecules to the emulsion/aqueous interface is not readily accomplished by traditional methods, for example, centrifugation is clearly not an option. However SHG measurements of adsorption to the emulsion/aqueous interface can be carried out. Measurements[63] of the adsorption of MG to a 230 nm diameter tetradecane−water emulsion using sodium dodecyl sulfate as the emulsifying agent yielded an adsorption free energy of -11.8 ± 0.5 kcal/mol. It should be noted that this free energy is within experimental error of the free energy of MG adsorbed to the PSS/aqueous interface, -11.1 ± 0.2 kcal/mol.[63] One possible explanation is that the surfaces of both PSS and the emulsion have the same terminal groups, namely, sulfate. Alternatively, this finding suggests that the interactions (electrostatic and others) of MG with the interfacial sulfate groups determine the MG adsorption free energy. The reasons that the adsorption free energy of MG to the PSS/aqueous interface differ by 1.6 kcal/mol from later work reported in the previous section are not presently known. A possible factor is the different companies that were used to supply the PSS spheres. This could lead to somewhat different sizes, size distributions, and charge densities between the PSS spheres used in the two laboratories.

2.7. Angular Patterns of SHG Scattering

Unlike linear light scattering, which is well understood and has proven to be a valuable tool[54,55,80−82] to characterize systems such as polymer solutions, emulsions, and colloids, the characteristics of nonlinear light scattering are just beginning to be probed.[83] One such effort[83] addressed the detection and analysis of the SH angular patterns due to colloidal particles. In these first experiments[83] of the angular second harmonic scattering properties of microspheres, a solution containing 1 μm polystyrene (PSS) microspheres and MG adsorbed to the PSS surface was used. The measurements revealed significant differences between the linear and the second harmonic scattering. One was the appearance of secondary peaks in the SHG scattering and the absence of exact forward scattering as seen in Figure 4.

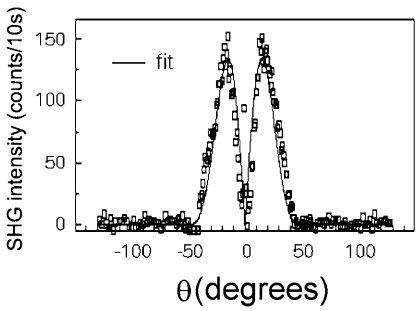

Figure 4. SHG scattering angular profile for 700 nm diameter particles and fitting (solid line). Incident light was s-polarized and SH was p-polarized. Reprinted from ref 82. Copyright 1981 Dover Publications.

Theoretical treatments of SHG scattering were found to be in accord with these experimental results.[83,84] In addition, it was found that the angle-resolved SHG scattering data for the 1 μm PSS−MG system could be described by a nonlinear analogue of linear Rayleigh−Gans−Debye scattering from microspheres as shown by the excellent fit (Figure 4).[83] A potentially useful characteristic of angle-resolved SHG measurements is the anisotropic scattering pattern generated by the surface of the microsphere. This anisotropic pattern has the potential to be used to differentiate SHG generated at the microsphere/aqueous interface from SHG generated in the bulk. For example, one can use the interesting finding that there is no s polarized SHG scattering from microsphere/aqueous interfaces.

The p and s polarized SHG scattering from a solution of nano- or microparticles is defined such that for light propagating in the plane of this page, the p polarized light is polarized in the plane of the page and the s polarized light is polarized in the plane perpendicular to this page. For a planar surface, the definitions are different. If this page is the surface plane, then the light polarized in the surface plane is s polarized (horizontal) and light polarized in the plane perpendicular to the surface plane is p polarized (vertical).

2.8. Air/Water Droplet Interface

The characterization of the aqueous interfaces of droplets and sprays in terms of their chemical composition, size,

charges, polarity, etc. is important for many reasons, among which are their effects on atmospheric chemistry. Various nonlinear optical processes (not SHG or SFG), for example, stimulated Brillouin scattering, stimulated Raman scattering, and third-order sum frequency generation measurements[85,86] of the bulk properties of droplets have proven to be useful. However information of their surface properties, which control the entry and departure of chemical species from the droplet bulk, is needed as well. The investigation of the interfacial properties of these important moieties was advanced by the first SHG measurements[87] of the surface of individual 1 mm diameter water droplets. The droplet interface had a population of surfactant molecules containing strongly nonlinear styryl dye molecules. The SH signal varied quadratically with the intensity of the incident light, as expected, but it was the dependence of the SHG intensity on the size of the droplet that showed that the SHG was generated coherently. By decrease of the size of the drop, while the number of surfactant molecules was kept constant, the surface density increased linearly with area, that is, varied as $1/r^2$, where r = radius of the droplet. For coherent scattering, the SHG varies with the square of the surfactant density, that is, SHG varies as $1/r^4$. This is exactly what was found, that is, SHG continues to be generated down to very small sizes as explained at the end of section 2.1.

3. Nanoparticles

The ability to control the optical and electronic properties of metallic nanoparticles by changing their size and shape has led to a significant number of applications, for example, catalysis, molecular electronics, and biosensing.[88,89] Investigations of[90,91] their linear optical properties are extensive and are generally understood, but as noted earlier, investigations of the nonlinear optical properties of small particles, nano- to microsize, are fairly recent. In this issue, which focuses on aqueous interfaces, it is the nanoparticle/aqueous interfaces that will be considered now. It should be recognized that there is a significant body of work on nanoparticles in other media, which are not included in this article.

3.1. Metallic Nanoparticles—Silver and Gold—Experiments and Theory

3.1.1. Silver Nanoparticles

A study[92] of 32 ± 6 nm diameter silver colloids in an aqueous solution revealed, for the first time, that there are both electric dipole and electric quadrupole contributions to the SHG signal. It was found that the optical nonlinearity of the silver nanoparticles is substantially greater than that of the "best" organic molecules, perhaps because of surface plasmon resonances at the second harmonic wavelength. The observed wavelength dependence of the SHG signal[92] was shown to be in agreement with theoretical treatments[84,93] of coherent SHG from centrosymmetric metallic nanospheres. In Figure 5, we see two peaks in the SHG scattering and the fitting of the data to two theoretical models.[84,93] The two peaks were attributed to surface dipole and quadrupole plasmon resonances with the quadrupole at higher energy. The chief difference between the two theories is that one of the theories was more general in including an additional surface contribution to the SHG, namely, the contribution due to a quadrupole excitation in the incident field. The more general theory gives a somewhat better fit to the data in the magnitude of the higher energy (shorter wavelength) peak arising from the quadrupole contribution.

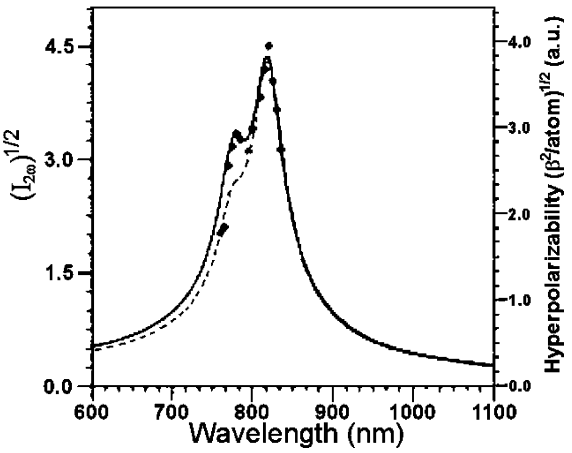

Figure 5. Second harmonic electric field and hyperpolarizability of silver colloid as a function of incident wavelength. Solid squares are the experimental data. The solid line is a fit to one theory[84] and the dashed line to a second theory.[93] Reprinted with permission from ref 92. Copyright 2002 American Institute of Physics.

It is clear that the development of SHG as a tool to investigate centrosymmetric nano- and microparticles has been advanced by a significant number of theoretical investigations.[84,93−99] One might ask at this point what is the value of the SHG studies, especially in relation to the much more widely used linear Rayleigh scattering. The value of SHG is that it yields information about a different part of the system than linear Rayleigh scattering. Linear Rayleigh scattering probes chiefly the bulk region of the particle, whereas SHG and SFG probe the surface region of the particle. Clearly a full description of chemical, physical, and biological properties requires information on both regions of the particle.

3.1.2. Gold Nanoparticles

An interesting finding in experiments[100] on 13 nm gold particles in aqueous solution was the marked difference in the effects of electrolyte concentration on hyper-Rayleigh, that is, incoherent SHG, and linear Rayleigh scattering (Figure 6).

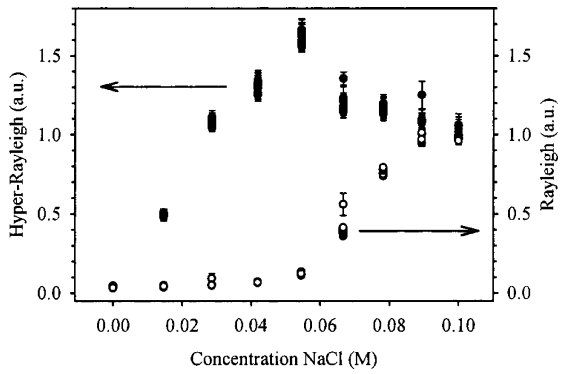

Figure 6. Effect of NaCl on linear Rayleigh and hyper-Rayleigh scattering intensities. Reprinted with permission from ref 100. Copyright 1998 American Chemical Society.

A factor that is relevant to the aforementioned result is that the concentration of electrolyte in a colloidal solution affects aggregation of the colloids. A consequence of aggregation of the gold colloids is the change in the surface

profile from a centrosymmetric nanosphere to an aggregate that can be centrosymmetric or not. The strong dependence of SHG on aggregation has been attributed[100] to the formation of a noncentrosymmetric entity, which could enhance the SHG intensity. Another possible factor is that the surface electronic structure is changed without making the component colloids in the aggregate noncentrosymmetric. At low electrolyte concentration, the coherent sum of the SHG is confined to individual colloids. However at high electrolyte concentrations, the coherent sum is over the colloids comprising the aggregate rather than the single colloids. The coherent SHG from an aggregate of microspheres should be considerably different than the coherent SHG from a single microsphere. An interesting comparison[100] of the SHG signal from nanosize gold colloids with suspensions of similar size, wide gap semiconductors, and insulator particles showed that the gold nanoparticles yielded an SH signal that was 10^5 stronger, an impressive difference. As with other metallic particles,[92,101] the origin of this marked difference is attributed to the resonant enhancement that occurs when the incident frequency or the second harmonic frequency is isoenergetic with plasmon frequencies of the metallic particle. This very strong plasmon resonant enhancement is well-known in other spectroscopies.[102−104] As we shall see, SHG is a sufficiently sensitive spectroscopy that plasmon resonances are not required to detect SHG signals from insulator nanoparticles.

3.1.3. Silver−Gold Hybrid Nanoparticles

The nonlinear optical properties of a novel metallic nanoparticle consisting of a gold core covered with a silver shell have been investigated.[101] The diameter of the pure gold core was 16 nm, and on addition of the silver shell, the diameter increased to 17−21 nm. It was reported that the SHG from the hybrid nanoparticles is increased by the SHG plasmon resonances, whereas for the linear Rayleigh scattering, there is an interplay between the surface plasmon resonance and interband transition resonances. The "hyperpolarizabilities" measured at different energies were found to increase with silver content at one energy and decrease for another energy. This was explained by shifts in the plasmon resonance with respect to the wavelengths at which the hyperpolarizabilities were measured. In discussion of the results of SHG scattering, it should be kept in mind that part of the SHG arises from a nonlocal electric dipole,[84,97,99] which means that there is not a rigorously defined hyperpolarizability, but rather some effective "hyperpolarizability" that could be helpful in comparisons of material nonlinearities.

3.1.4. Silica Nanoparticles

Among the more abundant and therefore significant mineral oxides in our environment is silica, SiO_2. The chemical properties[105−108] of microsized SiO_2 particles, an important component of soil, depend crucially on its surface charge. It is the acid−base chemistry of −SiOH surface groups in contact with the aqueous environment that determines the surface charge of the silica microparticles. The populations and identities of adsorbates and the orientational structure of adsorbed molecules at the interface are strongly influenced by interfacial electrostatics. An issue of keen interest is how the size of the microparticle affects its interfacial properties. An SHG study[109] that provides some information on this question used 10 nm diameter amorphous silica particles suspended in an aqueous solution. It was found that there are notable differences in the interface properties at a nanoparticle/aqueous interface[109] and a planar amorphous silica/aqueous interface.[110,111] The silica nanoparticle/aqueous interface study[109] showed that the SHG signal increased slightly with increasing electrolyte concentration. This was opposite to the observation[111] of a sharp decrease in SHG with increasing electrolyte concentration for a planar silica/aqueous interface. Another difference between the nano and planar aqueous interfaces was the pH dependence of the SHG signal. The results in the planar interface study[111] showed the presence of two acid−base equilibria; one was at $pK_a = 4.5$ for 20% of the silanols (−SiOH), and for the remaining 80%, $pK_a = 8.5$. The two different silanol sites could be due to one type of site where the silanols are hydrogen bonded to neighboring silanols, and for the other sites, the silanols are hydrogen bonded to water.[108] From the silica nanoparticle SHG vs pH data,[109] one cannot readily conclude that there are two different sites (Figure 7).

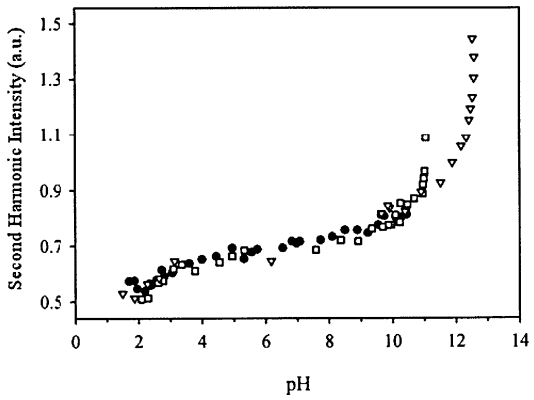

Figure 7. Dependence of the second harmonic intensity on pH for a colloidal silica solution (●, □, and △ indicate three different dilution-corrected experiments that have been normalized in the mid-pH region). Reprinted with permission from ref 83 (http://link.aps.org/abstract/PRL/v87/e103902). Copyright 2001 American Physical Society.

The different sites could be present but not separable in SHG experiments of the nano silica particles. The authors explain their nanoparticle results by changes in the hyperpolarizabilities due to changes in the nonresonant transition energy as the degree of protonation changes with pH.[109] This interpretation is supported by the correlation of the observed change in the SHG with the change in the number of the two different silanol sites. This latter quantity was extracted from IR and NMR studies.[108] The issue remains as to why there are such marked differences between the nano and planar interfaces. Because the next section, Electrostatic Potential at Charged Microparticle Interfaces, is relevant to these different findings, we will postpone discussion until after the next section is presented.

4. Electrostatic Potential at Charged Microparticle Interfaces

The surface charge density σ and the associated potential $\Phi(0)$ are important characteristics of planar and microscopic particle interfaces. They affect the populations and the structural arrangements of neutral and ionic species at the interface, interfacial chemical reactions, for example, acid−base chemistry, the electrokinetic properties of the particle, and the stability of colloidal suspensions.[54,55,77] SHG provides a noninvasive way for determining interfacial potentials[110−114] that is complementary to traditional methods.[54,55,77] For

nonconducting particles, the conventional method[54,55,77] involves measurement of the velocity of the particle in an electrostatic field applied across the aqueous solution. This method is called electrophoresis.[54,55,77] The electric potential obtained by electrophoresis is not the electrostatic potential at the surface of the microparticle but rather the potential, which is called the zeta potential, ζ, at the shear plane. The location of the shear plane is the boundary that separates the mobile fluid and the stationary shells of electrolyte and solvent molecules that move together with the particle. The ζ potential is always less than the potential at the surface of the particle because it is at a greater distance from the charged microparticle surface. Other methods for measuring interfacial electrostatic potentials include pH indicator molecules,[115−117] fluorescent yield measurements,[118] and atomic force microscopy.[119] All of these methods are of considerable value, but have difficulties because they perturb the microparticles, and because the locations of probe molecules in the interfacial region are not known, the electric field at a specified location is not known. SHG measurements[111] of the surface potential have been shown to be feasible based on the discovery that there are two contributions to the SHG signal. One contribution is from the second-order, $\chi^{(2)}$, susceptibility, and the other contribution is from the third-order $\chi^{(3)}\Phi(0)$ term. See eq 9. The $\chi^{(2)}$ contribution comes from the oriented chemical species at the interface, which are characterized by their second-order polarizabilities, $\alpha^{(2)}_{ijk}$, that is, their hyperpolarizabilities. The $\chi^{(3)}\Phi(0)$ contribution consists of the third-order nonlinear polarizabilities, $\alpha^{(3)}_{ijkl}$, of the chemical species in the bulk solution and also from bulk water molecules partially aligned by the electric field of the charged interface. The electrostatic field, which extends into the bulk solution, breaks the isotropy of the bulk solution. Consequently, SHG becomes electric dipole allowed for the bulk molecules, chiefly water molecules, that are polarized by the electric field. The electric field can extend from distances of tens of angstroms to hundreds of angstroms into the bulk aqueous solution depending on the electrolyte concentration. The total nonlinear polarization, $P^{\text{total}}_{2\omega}$ is equal to the sum of the second-order $P^{(2)}_{2\omega}$ and third-order polarization $P^{(3)}_{2\omega}$

$$P^{\text{total}}_{2\omega} = P^{(2)}_{2\omega} + P^{(3)}_{2\omega} \tag{7}$$

Expressing the polarizations in term of their susceptibilities and the incident light field at ω gives

$$P^{\text{total}}_{2\omega} = \chi^{(2)}E_\omega E_\omega + \chi^{(3)}E_\omega E_\omega \int_0^\infty E(r)\,\mathrm{d}r \tag{8}$$

where E(r) is the electric field at a distance r from the charged microparticle surface, and the assumption is made that $\chi^{(3)}$ does not depend on r. The electric field is integrated over the distance coordinate r to include the contributions to $P^{\text{total}}_{2\omega}$ from the bulk water molecules that are polarized by $E(r)$. The relation between the electric field and electric potential gives

$$P^{\text{total}}_{2\omega} = \chi^{(2)}E_\omega E_\omega + \chi^{(3)}E_\omega E_\omega \Phi(0) \tag{9}$$

where the reference potential at ∞ is set equal to zero and $\Phi(0)$ is the electrostatic potential at the charged surface. A successful model of the electrostatic potential of a planar charged surface in contact with an electrolyte solution is the Guoy−Chapman model.[54,55,77] This model is an exact solution of the Poisson−Boltzmann equation, which has proven[120−123] to be valid at low electrolyte concentrations, $<10^{-1}$ M, although it may be reasonable at higher concentrations.[124,125] The dependence of the interface electrostatic potential, $\Phi(0)$, on the electrolyte concentration can be seen in the Guoy−Chapman equation. It is

$$\Phi(0) = \frac{2kT}{Ze}\sinh^{-1}\left(\sigma\sqrt{\frac{\pi}{2\epsilon kTC}}\right) \tag{10}$$

where σ is the surface charge density, Z is the valence of the electrolyte, C is the concentration of the electrolyte in the bulk solution, and ϵ is the dielectric constant of the bulk solution. The dependence of the interface potential $\Phi(0)$ results from the electrolyte screening of the bulk water molecules from the charged interface. The dependence of the second harmonic field $E_{2\omega}$ on electrolyte concentration, shown in eqs 9 and 10, makes it possible to test the Guoy−Chapman model in a straightforward way.[110,111] The measurements[110,111] of the dependence of the SH signal on electrolyte for planar aqueous interfaces were found to be in good agreement with that predicted by the Guoy−Chapman model.[110,111] Similarly, in SHG studies[126] of

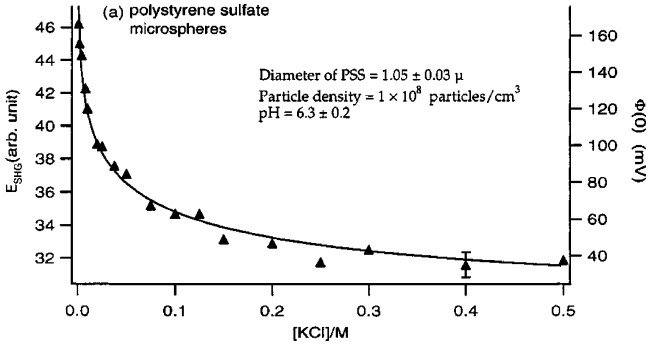

Figure 8. Second harmonic field and surface potential, $\Phi(0)$, plotted as a function of KCl concentration for polystyrene sulfate microspheres in aqueous solution. The triangles are the experimental data. The solid curve is a fit to the Guoy−Chapman model. Reprinted in part from ref 126 with permission. Copyright 1998 American Chemical Society.

charged microspheres, the dependence of the SH signal on electrolyte was also found to be in good agreement with the Guoy−Chapman theory (Figure 8).

The charged microparticles were PSS beads and emulsion oil droplets suspended in aqueous solutions.[126] The negatively charged PSS had a diameter of 1 μm and a density of 10^8/cm^3. The emulsion droplets had a diameter of 0.2 μm and a density of (6×10^{10})/cm^3. The absolute values of the interface electrostatic potentials were in the range of 40−220 mV depending on the electrolyte concentration. The use of the planar surface Guoy−Chapman expression of $\Phi(0)$ for the spherical microparticles was shown to differ by less than 4% from an exact numerical calculation.[126] Using results obtained from SHG and electrophoresis measurements,[126] a comparison of the potentials obtained was carried out. The SHG values for $\Phi(0)$ were determined to be -120 ± 11 mV for PSS in a 0.01 M KCl solution and -62 ± 10 mV for a 0.1 M KCl solution.[126] The values of the ζ potentials obtained[126] at 0.01 M KCl and 0.1 M KCl were -73 ± 5 and -37 ± 3 mV, respectively. The differences between the values of the ζ potential obtained by electrophoresis and the potentials obtained by SHG are a consequence of the fact

that the ζ potential is the value of the electrostatic potential at the location of the shear plane, which is at some distance from the charged surface of the PSS microsphere. The SHG derived potential is the potential at the charged plane.

In 1961, long before second harmonic spectroscopy, a theory was developed[127] that related the potential $\Phi(0)$ at the charged surface to the ζ potential. Putting the SHG experimental values obtained in the PSS microparticle studies into this theory made it possible to calculate the values of the ζ potentials. The predictions[126] were -75 and -35 mV at 0.01 and 0.1 M electrolyte concentrations, respectively. These predicted ζ potential values are in excellent agreement with the measured[126] values of the ζ potentials, -73 ± 5 and -37 ± 3 mV.[126] The agreement between theory and experiment provides strong support for the theoretical model.[127]

At this point, we return to the earlier discussion of the sharp difference in the aqueous interface properties of 10 nm amorphous silica nanoparticles[109] and that of planar amorphous silica.[111] A crucial factor that can be responsible for the observed nano vs planar properties is the concentration of the silica nanoparticles suspended in the aqueous solution. Under the reported[109] conditions of the SHG experiments, the concentration of the nanoparticles was 0.27 M, which is a very high concentration. It should be noted that silica gels are also at a high silica density. The 0.27 M nanoparticle concentration corresponds approximately to a nanoparticle density of 1.6×10^{20} particles/cm^3 or about 6×10^3 Å^3/particle and a center−center distance of about 10 Å. The water and electrolytes separating the nanoparticles in this confined space cannot be described as isotropically distributed. The $\chi^{(2)}$ contributions to the SHG signal from the noncentrosymmetrically distributed water molecules located between the nanoparticles and the high interfacial density of neutral $-$SiOH and charged $-SiO^-$ groups could be significantly larger than the $\chi^{(3)}\Phi(0)$ contributions from the noncentrosymmetrically distributed water molecules located between the nanoparticles. On the other hand, for the planar silica/aqueous interface, a very large number of isotropically distributed water molecules in the bulk solution are polarized by the charged surface. This results in contributions from the partially aligned water molecules to $\chi^{(3)}\Phi(0)$ and the contributions originating from the third-order polarizabilities, $\alpha^{(3)}_{ijkl}$, of the bulk water molecules. It is necessary to determine how these arguments can explain the different SHG dependences on electrolyte concentration. A consideration that is relevant to the silica nanoparticle and planar silica experiments were studies on silica gels, which found that the density of negatively charged sites, that is, $-SiO^-$, increased as the electrolyte concentration increased.[128,129] This increase in ionization of the silanol groups as electrolyte concentration increases can be attributed to the increase in the Debye screening, which decreases the repulsive interactions between $-SiO^-$ groups. If the Debye screening affects the nanoparticle suspensions, what about the Debye screening effect on the planar silica aqueous interface? Just as with the nanoparticles, the repulsions among the surface $-SiO^-$ groups would be decreased by an increase in the electrolyte concentration. This would favor the ionization of additional silanol groups, which would yield more charged $-SiO^-$ groups. As a consequence, the surface potential would become more negative with increasing electrolyte concentration. The SHG experiments found[111] that the potential decreased, that is, became less negative, not more negative. It was concluded therefore that the electrolyte dependence of the SHG signal from the planar silica interface was dominated by the polarization of bulk water molecules as expressed by the $\chi^{(3)}\Phi(0)$ term. In other words, electrolyte screening of bulk water molecules from the charged surface, which is expressed in the $\chi^{(3)}\Phi(0)$ term, is more important than the electrolyte screening of the repulsive $-SiO^-$ interactions, which is expressed in the $\chi^{(2)}$ term, in determining the SH signal from the planar silica/aqueous interface. We can speculate that the different dependencies of SHG on electrolyte concentration for the nanoparticle and planar interfaces arises from different terms contributing to the SH signal (see eq 9). At the high densities of the nanoparticle experiments, the contribution could come chiefly from $\chi^{(2)}$, which is dependent on the anisotropically distributed water molecules and on the hyperpolarizabilities of the $-$SiOH and $-SiO^-$ groups. The electrolyte concentration affects the fraction of silanols ionized and in that way the value of $\chi^{(2)}$. If this line of reasoning is correct, it predicts that the hyperpolarizability of the ionized form is larger than that of the neutral form because SHG is observed to increase with electrolyte concentration in the nanoparticle experiments. The SHG results for the planar silica/aqueous interface indicate that the electrolyte dependence of the SH signal is dominated by the $\chi^{(3)}\Phi(0)$ term. These considerations, if correct, can explain the marked differences between the nanoparticle/aqueous and planar/aqueous experimental findings.

5. Clay Particle/Aqueous Interface

The abundance and the unique adsorptive and catalytic properties of clay make it a substance of fundamental and technological importance.[130,131] It has been used for a long time as a catalyst in petroleum-forming reactions and because of its large surface area as an adsorbent in the removal of organic pollutants from aqueous media.[132] It has also been recognized that clays may have contributed to the chemical evolution of organic compounds involved in the origin of life.[133] The electrostatic characteristics of clay microparticles play a key role in soil chemistry.[55,130−132] SHG studies[134] of centrosymmetric disk-shaped montmorillonite particles suspended in water with a diameter 0.5 μm and a thickness of 0.01 μm have been performed. Since the diameter is on the length scale of the light and the thickness is much smaller than the wavelength of the light, the edge surfaces, separated by 0.5 μm, can contribute to the SHG signal, whereas the contribution of the large planar surfaces is diminished because of their small separation, 0.01 μm. The SHG signal of the bare clay/aqueous interface contains contributions from the surface second-order nonlinearities and also from the electric field oriented water molecules near the charged edge surface. In addition to detecting the clay/aqueous interface, the adsorption of the organic dye molecule 4-(2-pyridylazo)-resorcinol (PR) by the clay particles was observed.[134]

6. SH Spectrum of a Charge-Transfer Complex on Semiconductor TiO_2 Microparticles

TiO_2, a wide band-gap semiconductor, has been studied extensively because of its special chemical and physical properties and its potential utility in solar energy conversion and photocatalysis.[135−147] Colloidal particles of anatase (a noncentrosymmetric form of TiO_2 crystal) are widely used because it is easy to obtain and also to take advantage of the high specific surface area available in the dispersed small

particles. For wide band-gap semiconductors, such as TiO_2, the energy gap is too large to efficiently use the output of the sun.

Because of this, surface photosensitization of TiO_2 is a very important process in solar energy conversion, see Scheme 3. Catechol, *o*-hydroxy phenol, is known[146,147] to

Scheme 3

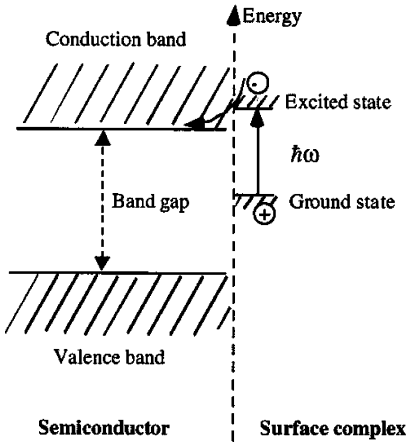

form charge-transfer complexes with the −TiOH surface groups. The spectrum of the complex extends into the visible region and provides a good overlap with the solar spectrum. The absorption of light in the visible region has the desired effect of injecting electrons into the conduction band of TiO_2. The complex between catechol and TiO_2 has been previously studied by UV/vis absorption measurements[147] on 30 nm TiO_2−catechol dried powders and in 13 nm TiO_2−catechol particles in a methanol−water mixture.[146] Using SHG spectroscopy, the charge-transfer band of the surface complex of catechol on TiO_2 colloid particles (anatase, 400 nm) at low particle density ($4 \times 10^8/cm^3$) in aqueous suspension was obtained (Figure 9).[148]

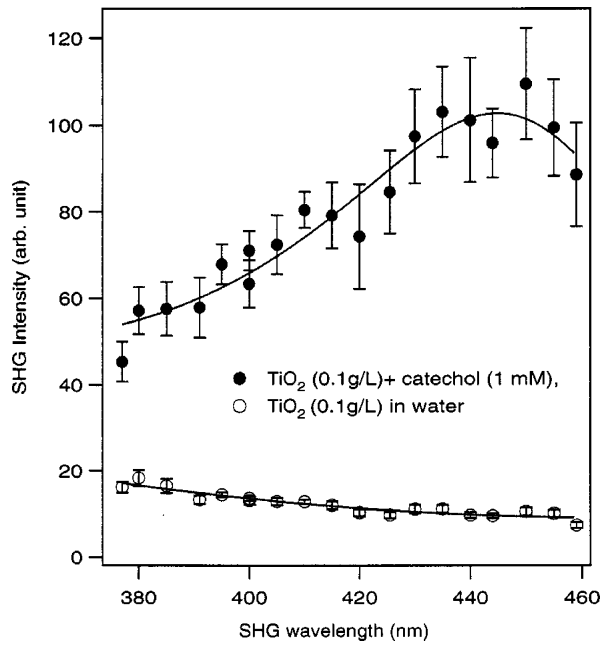

Figure 9. The turbidity-corrected and normalized SH spectra of TiO_2 in water and TiO_2 in 1 mM catechol solution. The peak of the catechol−TiO_2 surface complex band is at $\lambda_{max} = 456 \pm 4$ nm. Reprinted with permission from ref 148. Copyright 1999 American Chemical Society.

The charge-transfer band of the catechol−TiO_2 complex was centered at 2.72 eV (456 nm). The diffuse reflectance spectra[147] of the 30 nm dried powder displayed a shoulder at 420 nm. The aqueous methanol measurements[146] showed a broad featureless spectrum (Figure 10). The free energy

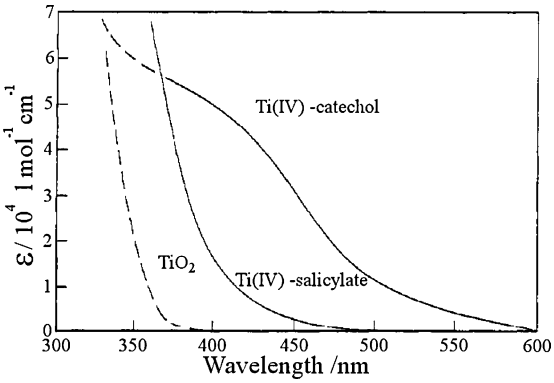

Figure 10. UV−vis absorption spectra of TiO_2 transparent sols (0.5 g/L, pH 3.6). ϵ is the absorption coefficient for the various TiO_2 systems. Reprinted with permission from ref 146. Copyright 1991 American Chemical Society.

of adsorption obtained[148] from SHG measurements of the low-density TiO_2−catechol/aqueous system was $\Delta G° = -4.6$ kcal/mol. The free energy values obtained using separation methods were $\Delta G° = -6.8$ kcal/mol[146] and $\Delta G° = -5.4$ kcal/mol.[147] In the experiments, other than the SHG ones, it was necessary to use very high particle densities, which makes interpretation more difficult because of particle−particle interactions. The differences in the systems, for example, nano- vs microparticle and aqueous vs aqueous−methanol, and possible aggregation of the TiO_2 nanoparticles at the high densities used in the separation measurements that are orders of magnitude higher than the densities used in the microparticle SHG measurements, could easily be responsible for the variations in the free energies.

We will now consider the effects of the anatase form of TiO_2 not having a centrosymmetric structure. It is now necessary to include the contribution of the bulk region of the microparticle as well as the contribution from the surface adsorbed species to the SHG signal. If we were considering macroscopic size anatase, then the bulk contribution to the SHG signal could dominate the contribution of the surface adsorbed molecules. For a suspension of anatase microparticles, the large surface area occupied by the molecular adsorbates can be comparable to or even greater than the bulk contribution. Measurements at wavelengths far from bulk resonances but close to surface molecular resonances can be used to enhance the surface vs bulk contribution. To separate the contributions of the surface and bulk to the signal, the relative phase of their second harmonic electric fields were measured. In this way, the surface charge-transfer spectrum was obtained. Anatase microparticles were selected for study rather than the centrosymmetric rutile form of TiO_2 to demonstrate that the surface adsorbate contributions could be determined for noncentrosymmetric particles as large as 0.4 μm. In addition, the SHG study of anatase made it possible to compare the SHG measurement of the catechol−TiO_2 charge-transfer spectrum with previous linear experiments that were carried out on catechol−TiO_2 anatase systems.

7. Liposomes

One fascinating class of centrosymmetric particles are liposomes. These microparticles are of widespread interest as biological membrane mimetic structures, as drug delivery systems, and as possible structures in solar energy conversion systems.[149−151] The basic structure of a liposome is a bilayer made up of amphiphiles that self-assemble into a spherical structure with an enclosed aqueous compartment, Scheme 4.

Scheme 4

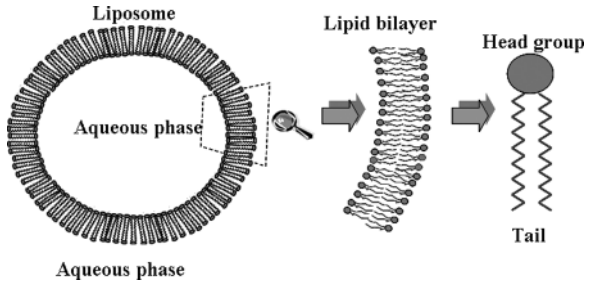

The two monolayers comprising the bilayer have the hydrophobic alkane chains facing each other with the polar headgroups projecting into the internal aqueous region and the other into the external aqueous region. Liposomes serve as membrane mimetic structures because the basic structure of a biological membrane is a bilayer in which the amphiphiles are phospholipids. It is the membrane that determines the identities and population of chemical species adsorbed to the membrane/aqueous interface, as well as control the passage of adsorbed species and electrical signals between the inside and the outside of a cell. With liposomes one can vary and thereby investigate how the phospholipid composition affects the free energies of adsorption, the electrostatic potential at the interface, and, as will be discussed, the transport of chemical species across the bilayer.

7.1. Molecular Transport across a Membrane in Real Time

Just as SHG has been used to investigate equilibrium properties of liposomes such as adsorption free energies,[152] effects of surface charge on adsorption,[152] and interface potentials,[153] it can also be used to measure their time-dependent properties.[64,152,154−156] In particular a SHG method has been developed to observe molecules crossing the liposome bilayer in real time.[64,152,154−156] The idea of the method is based on the recognition that molecules adsorbed on the outer surface of a liposome are oriented in a preferred way, and by symmetry the same molecules when adsorbed on the inner surface of the liposome would have the opposite orientation.

The method is briefly described. Following the rapid mixing (<1 s) of an aqueous solution containing liposomes with an aqueous solution containing an organic solute such as malachite green, MG, a rapid (<1 s) diffusion and adsorption to the outer surface of the liposome takes place. The adsorbed MG molecules were observed to yield a strong SHG signal. If the organic molecule permeates across the bilayer, then it would have an orientation that is opposite to its orientation at the outer surface. Because the thickness of the bilayer is small, ∼4 nm, the second harmonic polarizations of the oppositely oriented molecules on the inner and outer surfaces would cancel. Thus as molecules cross the bilayer the strong initial SHG signal would decay in time. The magnitude of the SHG electric field, $E_{2\omega}$, at a time t after mixing is linearly proportional to the difference in the populations of MG on the outer surface and inner surface at time t.

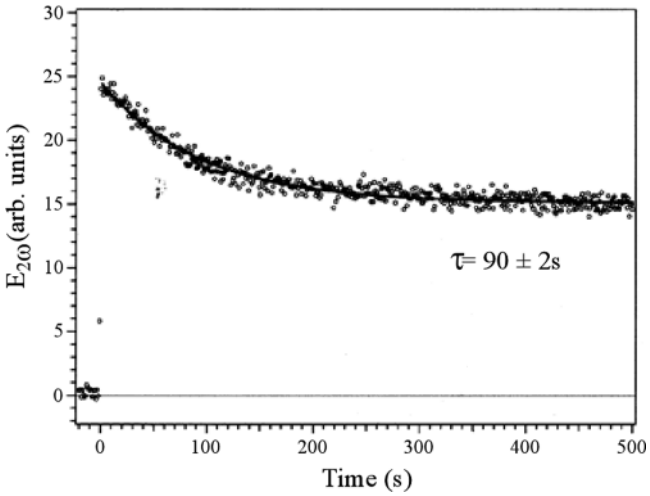

Figure 11. Second harmonic field, $E_{2\omega}$, following mixing of the DOPG liposome solution with the malachite green, MG, solution at time $t = 0$. Reproduced from ref 156 by permission of The Royal Society of Chemistry.

Figure 11 shows the transport kinetics of MG crossing the bilayer of a 100 nm dioleoylphosphatidylglycerol (DOPG) negatively charged liposome.[156] It should be noted that biological cells are usually negatively charged because negatively charged phospholipids are part of the membrane structure.[149] Similarly many drugs and peptides that cross membrane bilayers are cationic, as is MG.[149,157,158] The SHG method is complementary to other techniques because it is a surface technique sensitive to both the inner and outer surfaces of the membrane bilayer. This is generally not the case with other methods, which must distinguish molecules adsorbed at the inner and outer membrane surfaces, as well as molecules in the bulk aqueous solution. In other methods, for example, NMR, EPR, fluorescence, it is often necessary to introduce extraneous probe molecules to determine that a molecule has permeated across the bilayer.[159−164] Among these probe molecules are fluorescence quenchers, shift reagents, and spin labels. Some techniques require precise calibration of microenvironment signal changes to determine the location of the molecule, inside or outside the liposome. There are of course difficulties with the SHG method as indicated earlier.

Other experiments[165] on the transport of an adsorbate from the outer monolayer to the inner monolayer employed a neutral styryl dye and a neutral dioleoylphosphatidylcholine (DOPC) liposome. The SH signal decayed with time as dye adsorbates crossed from the outer leaf to the inner leaf of the liposome (Figure 12). The liposome used is quite different in size from typical liposomes, which are of the order of 100 nm diameter; the DOPC liposome is tens of micrometers in diameter. Similarly the charges of the transport molecules are different; MG is positively charged and the styryl dye is neutral. The thickness of the bilayer, which is the important parameter in transport across bilayers, is the same ∼4 nm as in most other liposomes. The SH signal decay time of 2 h is significantly longer than the ∼90 s for MG, due perhaps

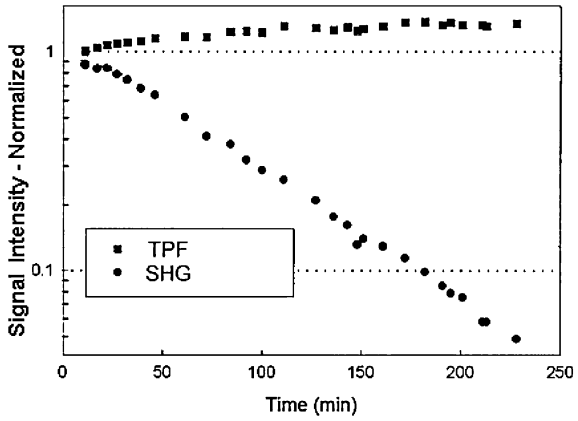

Figure 12. The dynamics of styryl dye flip-flop in a POPC liposome initially labeled in the outer leaflet: SHG (●) and two photon fluorescence TPF (■). The time constant for the styryl dye flip-flop at room temperature is about 2 h. Reprinted with permission from ref 165. Copyright 2001 Biophysical Society.

to the very much larger size of the styryl dye. A more interesting difference is the observation that the SH signal for the styryl dye approaches zero indicating that the dye populations on the inner and outer leafs have become approximately equal at long times. Unlike these observations, the experiments with the charged MG showed[156] that the SH signal did not approach zero at long times. Experiments to be presented in a later section offer an explanation of these findings.

7.1.1. Effects of Cholesterol on Transport Kinetics

Cholesterol is an essential constituent of plasma membranes in mammalian cells, ranging from 50% of the lipids in some membranes to a very low percentage in other membranes.[166] It has a pronounced effect on the physical properties of membranes, particularly on the structure of the phospholipid bilayers.[151,167−170] Its effects on transport kinetics of various chemical species across a liposome bilayer are important as a model of transport across the membranes of biological cells and in the use of liposomes as drug delivery systems.[151,171−177] SHG measurements[154] of the effect of cholesterol on the molecular transport of MG across DOPG liposome bilayers with 0−50 mol % cholesterol have been carried out. The experiments showed that the higher the cholesterol content the slower the transport. The transit time was found to increase by a factor of 6 in going from no cholesterol to 50% cholesterol. A possible mechanism responsible for this large effect assumes that the incorporated cholesterol molecules force the hydrocarbon chains of the phospholipids into a more ordered configuration, increasing the density, which decreases the fluidity and thereby reduces the permeability kinetics of molecules crossing the bilayer.[178]

7.1.2. Effects of Liposome Charge on Transport Kinetics

The capability to make liposomes that have different proportions of charged and neutral phospholipids provides a way to investigate the effects of membrane charge on both equilibrium and time-dependent processes. To this end, liposomes were made with negatively charged palmitoylphosphatidylglycerol (POPG) and the neutral lipid palmitoylphosphatidylcholine in various proportions. At 25 °C, the lipids mix ideally.[179] It was found in SHG experiments[153] that both the adsorption of MG and its bilayer crossing time were sensitive to composition. The adsorption equilibrium constant decreased by more than an order of magnitude as the POPG content was reduced from 100% to 25%. By variation of the fraction of the charged POPG lipid in the bilayer, it was found that the transport rate constant scaled linearly with the POPG content.

An interesting finding was the dependence of the transport rate constant on the concentration of MG. At the highest MG concentration (12μm) the rate constant was four times greater for the 100% POPG than its value at 25% POPG (Figure 13). However as the concentration of MG decreased,

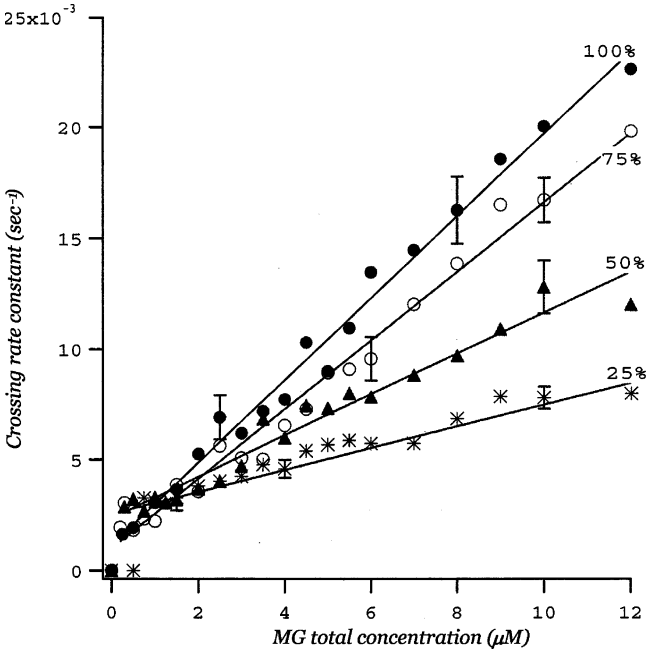

Figure 13. Effects of the percentage of the charged lipid POPG on the rate constant for crossing the bilayer of the hybrid POPC−POPG liposomes. The percentages refer to POPG. Reprinted with permission from ref 152. Copyright 2001 Biophysical Society.

the rate constants for the differently charged liposomes converged to the same value. This means that the transfer rate constant does not depend explicitly on the liposome charge, which if correct has important implications on the transport of organic ions across biological membranes. To understand why the bilayer charge markedly affects the transport at higher MG concentrations (10^{-5} M) but has no effect at lower MG concentrations ($\sim 10^{-6}$ M) requires a determination of whether MG adsorbs to both POPG lipid sites and POPC lipid sites or preferentially adsorbs to one type of site. It is known[152] from SHG experiments that MG adsorbs strongly to pure POPG liposomes and negligibly to pure POPC liposomes. Therefore the number of MG adsorbate sites scales directly with the percentage of POPG lipids in the hybrid POPC−POPG liposomes. At very low concentrations of MG in the bulk aqueous solution, $\sim 10^{-6}$ M, the MG adsorption by the liposome is small. Under these circumstances, there is such a large excess of POPG sites over MG adsorbates at both the lowest POPG percentage, that is, 25%, and at 100% POPG that the adsorbate population is determined by the bulk concentration of MG and not by the lipid composition of the hybrid liposomes. Consequently, the rate constants are the same for all compositions, as is observed. However as the bulk concentration of MG increases, up to a maximum of 12 μM, there is no longer a large excess of POPG sites with respect to MG adsorbates. As the percentage of POPG lipids increases

so does the number of sites for MG adsorption on the outer surface of the liposome. This results in an increased MG adsorption to the outer surface and, consequently, a larger MG concentration gradient across the bilayer. It is the concentration gradient that provides the driving force for crossing. The larger gradient at the higher POPG percentage leads to a larger rate constant for transport to the inner surface of the liposome. These considerations can explain both the independence of the MG crossing rate constant on liposome composition at low MG concentrations and the increase in the rate constant, which is dependent on liposome composition, at higher MG concentrations.

The preceding discussion however does not explain why the SH signal does not approach zero at long times, that is, why the MG populations on the inner and outer surfaces do not become roughly equal at long times. It turned out that electrostatic effects had to be considered to address this point. Because MG crosses the bilayer without its Cl^- counterion,[155] there is a buildup of positive charge on the inner surface. The development of a positive electrostatic potential in the inner compartment of the liposome opposes the crossing of additional MG, that is, makes it more energetically costly for MG to cross. The net transport of MG across the bilayer stops when the chemical gradient that drives MG across the bilayer comes into balance with the positive electrostatic potential that opposes the crossing of MG to the inner surface. It should be noted that the positive electrostatic potential inside the liposome depends only on the number of MG that have crossed to the inner surface and not on the MG adsorbate population. Therefore the electrostatic effect is the same at 25% POPG as at 100% POPG.

7.1.3. Antibiotic-Assisted Transport Kinetics

To test the idea that an electrostatic potential was responsible for the SHG signal not decaying to a value close to zero, as would be expected if the populations of MG on the inner and outer surfaces became roughly equal, experiments[156] were carried out to remove the electrostatic potential across the bilayer. To achieve this, a Na^+ ion transporter, which can transport Na^+ across the bilayer, was added to the liposome solution. A well-known lipophilic Na^+ ion transporter is the antibiotic valinomycin,[180,181] Scheme 5.

Scheme 5. Valinomycin

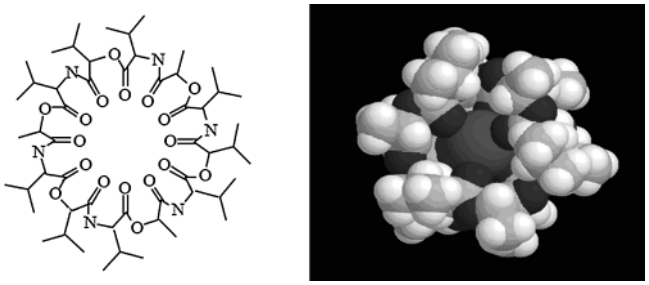

As MG crosses the bilayer, a positive potential develops inside the liposome, and therefore, a negative potential develops in the external solution. The negative potential favors the transport of Na^+ from inside the liposome to the external solution. This transport of Na^+ from inside to outside can compensate the positively charged MG that crosses to the inside compartment. The Na^+ transport prevents the formation of an inside positive potential that limits the MG permeation of the bilayer. The results shown in Figure 14

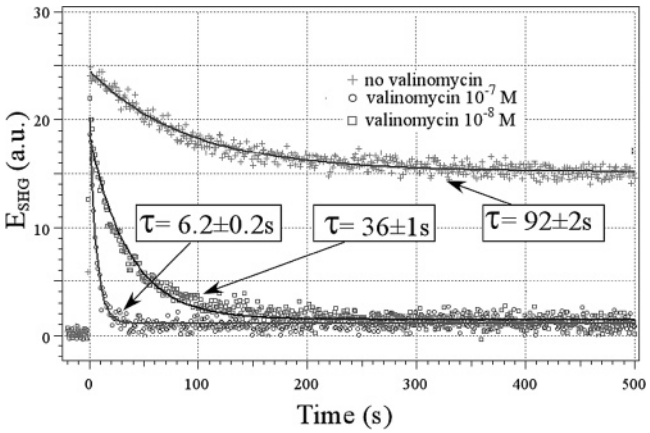

Figure 14. Effect of valinomycin on malachite green transport kinetics across a DOPG liposome bilayer. Reprinted with permission from ref 152. Copyright 2001 Biophysical Society.

demonstrate that the SHG signal approaches zero, indicating roughly equal populations at the inside and outside interfaces.

It was concluded therefore that the development of a positive potential inside the liposome was responsible for the slower crossing rate and for the populations of MG at the inner and outer surfaces of the liposome. Related to this discussion of the effect of an electrostatic potential on transport of MG across the DOPG bilayer is the study[166] described earlier in which the time dependence of a styryl dye moving from the outer monolayer to the inner monolayer of a DOPC liposome bilayer was measured. A notable difference from the MG results[156] with pure DOPG liposomes was the observation[166] that the SH signal approached zero at long times, Figure 12. The reason for the different behavior is the electrostatic potential that develops as MG crosses the bilayer, whereas no potential develops as the neutral styryl dye flip-flops from the outer surface to the inner surface of the liposome. Without the blocking electrostatic potential on the inner and outer monolayers, the populations of the styryl dye on the inner and outer monolayers can become roughly equal. The styryl dye orientation in the outer leaf is opposite to its orientation in the inner leaf because of symmetry. The second-order polarizations induced by the incident light have opposite phases because of their opposite orientations and cancel each other, and there is no SHG.

8. Summary

Hopefully the work discussed in this review has demonstrated the power of SHG spectroscopy to investigate the aqueous interfaces of nano- and microparticle systems. These systems extend from insulator and metal nanoparticles to semiconductor microparticles, water droplets, and membrane mimetic liposomes. There have been significant theoretical advances that connect the measurements of the SHG emanating from these particles with theoretical models of SHG and the sizes and material properties of these particles. Technologies have played their part in advancing the experiments that have been discussed in this review. It is surely impressive that the work described herein constitutes the development of a new research area within the time span of about 10 years. At this point, it might be of interest to speculate briefly about future directions of SHG and SFG investigations of nanoparticle and microparticle aqueous interfaces. It is clear that we need structural information on the organization of water molecules at the nano- and microparticle interfaces. Imagine

the diverse water structures associated with the vast array of nanoparticle shapes ranging from cubes to pyramids to many others. SFG studies of water vibrations and those of other interfacial species can have a major impact in advancing our understanding of the interactions among the various chemical species at numerous interfaces. The identification of the interfacial species, chemical reactions, and equilibria at these small particle interfaces, as well as the dynamics of molecular motion, energy relaxation, and photochemical processes, will more than likely be the subjects of many SHG and SFG studies. The chemistry and physics of these small particle interfaces, especially the many different structural forms of nanoparticles, are likely to offer an abundance of surprises. An increase in theoretical studies of interfaces would be of great value and will probably grow rapidly as new and challenging experimental results are reported. Technology advances in laser and detection apparatus will improve the sensitivity of these nonlinear measurements and make it possible to investigate phenomena and systems that are presently beyond our reach. Advances in computer technology and the development and availability of new software and programs will be invaluable in improved modeling of the data from interfacial experiments. Of course, the most exciting developments will be ones that we presently do not anticipate. If we look back 10 years, we might ask what were the unexpected developments. I leave this to the reader to ponder.

9. Acknowledgments

This work was supported by the National Science Foundation and by the Chemical Sciences, Geosciences and Biosciences Division, Office of Basic Energy Sciences, Office of Science, U.S. Department of Energy. The author thanks Dr. M. Comstock for his able assistance.

10. References

(1) Xu, P.; Wen, X.; Zheng, Z.; Kable, E.; Cox, G.; Zhu, H. *Proc. SPIE—Int. Soc. Opt. Eng.* **2005**, 5931.
(2) Fedyanin, A. A.; Aktisipetrov, O. A.; Kurdyukov, D. A.; Golubev, V. G.; Inoue, M. *Proc. SPIE—Int. Soc. Opt. Eng.* **2005**, 5480.
(3) Nuriya, M.; Jiang, J.; Nemet, B.; Eisenthal, K. B.; Yuste, R. *Proc. Natl. Acad. Sci.* **2006**, *103*, 786.
(4) Figliozzi, P.; Sun, L.; Jiang, Y.; Matlis, N.; Mattern, B.; Downer, M. C.; Withrow, S. P.; White, C. W.; Mochan, W. L.; Mendoza, B. S. *Phys. Rev. Lett.* **2005**, *94*, 047401.
(5) Liu, J.; Conboy, J. C. *Langmuir* **2005**, *21*, 9091.
(6) Wang, C. Y.; Groenzin, H.; Shultz, M. J. *J. Am. Chem. Soc.* **2005**, *127*, 9736.
(7) Gopalakrishnan, S.; Jungwirth, P.; Tobias, D. J.; Allen, H. C. *J. Phys. Chem. B* **2005**, *109*, 8861.
(8) Moran, A. M.; Sung, J. H.; Hicks, E. M.; Van Duyne, R. P.; Spears, K. G. *J. Phys. Chem. B* **2005**, *109*, 4501.
(9) Brehm, G.; Sauer, G.; Fritz, N.; Schneider, S.; Zaitsev, S. *J. Mol. Struct.* **2005**, *735*, 85—102.
(10) Welsh, A. H.; Mansson, R. A.; Frey, J. G.; Danos, L. *Chemom. Intell. Lab. Syst.* **2005**, *75*, 45.
(11) Simpson, G. J.; Dailey, C. A.; Plocinik, R. M.; Moad, A. J.; Polizzi, M. A.; Everly, R. M. *Anal. Chem.* **2005**, *77*, 215.
(12) Beildeck, C. L.; Steel, W. H.; Walker, R. A. *Faraday Discuss.* **2005**, *129*, 69.
(13) Yui, H.; Hirose, Y.; Sawada, T. *Anal. Sci.* **2004**, *20*, 1493.
(14) Bordenyuk, A.; Benderskii, A. V. *Abstr. Pap. Am. Chem. Soc.* **2004**, *228*, U204.
(15) Ortegren, J.; Wantke, K. D.; Motschmann, H.; Mohwald, H. *J. Colloid Interface Sci.* **2004**, *279*, 266.
(16) Nemet, B. A.; Nikolenko, V.; Yuste, R. *J. Biomed. Opt.* **2004**, *9*, 873.
(17) Zheludev, N. I.; Emel'yanov, V. I. *J. Opt. A* **2004**, *6*, 26—28.
(18) Petersen, P. B.; Saykally, R. J. *Chem. Phys. Lett.* **2004**, *397*, 51.
(19) Konek, C. T.; Musorrafiti, M. J.; Al-Abadleh, H. A.; Bertin, P. A.; Nguyen, S. T.; Geiger, F. M. *J. Am. Chem. Soc.* **2004**, *126*, 11754.
(20) Benjamin, I. *Chem. Phys. Lett.* **2004**, *393*, 453.
(21) Beermann, J.; Bozhevolnyi, S. I. *Phys. Rev. B* **2004**, *69*, 155429.
(22) Kongsted, J.; Osted, A.; Mikkelsen, K. V.; Christiansen, O. *J. Chem. Phys.* **2004**, *120*, 3787.
(23) McClelland, A.; Fomenko, V.; Borguet, E. *J. Phys. Chem. B* **2004**, *108*, 3789.
(24) Kataoka, S.; Gurau, M. C.; Albertorio, F.; Holden, M. A.; Lim, S. M.; Yang, R. D.; Cremer, P. S. *Langmuir* **2004**, *20*, 1662.
(25) Chen, C. Y.; Wang, J.; Loch, C. L.; Ahn, D.; Chen, Z. *J. Am. Chem. Soc.* **2004**, *126*, 1174.
(26) Holman, J.; Davies, P. B.; Neivandt, D. J. *J. Phys. Chem. B* **2004**, *108*, 1396.
(27) Dombeck, D. A.; Blanchard-Desce, M.; Webb, W. W. *J. Neurosci.* **2004**, *24*, 999.
(28) Makeev, E. V.; Skipetrov, S. E. *Opt. Commun.* **2003**, *224*, 139.
(29) Brudny, V. L.; Mochan, W. L.; Maytorena, J. A.; Mendoza, B. S. *Phys. Status Solidi C* **2003**, 518.
(30) Rao, Y.; Tao, Y. S.; Wang, H. F. *J. Chem. Phys.* **2003**, *119*, 5226.
(31) Millard, A. C.; Jin, L.; Lewis, A.; Loew, L. M. *Opt. Lett.* **2003**, *28*, 1221.
(32) Anceau, C.; Brasselet, S.; Zyss, J.; Gadenne, P. *Opt. Lett.* **2003**, *28*, 713.
(33) Downer, M. C.; Figliozzi, P.; Jiang, Y.; Sun, L.; Mattern, B.; White, C. W.; Withrow, S. P. *Proc. SPIE—Int. Soc. Opt. Eng.* **2003**, 5223.
(34) Pons, T.; Moreaux, L.; Mertz, J. *Phys. Rev. Lett.* **2002**, *89*.
(35) Richmond, G. L. *Chem. Rev.* **2002**, *102*, 2693.
(36) Chen, Z.; Shen, Y. R.; Somorjai, G. A. *Annu. Rev. Phys. Chem.* **2002**, *53*, 437.
(37) Opdahl, A.; Somorjai, G. A. *Langmuir* **2002**, *18*, 9409.
(38) Jorkaala, H.; Stennenen, H. *J. Opt. A* **2002**, *4*, 366—369.
(39) Williams, C. T.; Beattie, D. A. *Surf. Sci.* **2002**, *500*, 545.
(40) Briggman, K. A.; Richter, L. J.; Stephenson, J. C. *Opt. Lett.* **2001**, *26*, 238.
(41) Dapap, J. I.; Heinz, T. F. In *Encyclopedia of chemical physics and physical chemistry*; Moore, J. H. and Spencer, N. P., Eds.; Elsevier: Amsterdam, 2001.
(42) Neuendorf, R.; Brysch, A.; Bour, G.; Kreibig, U. *Proc. SPIE—Int. Soc. Opt. Eng.* **2001**, 4456.
(43) Mitra, A.; Thareja, R. K. *Mod. Phys. Lett. B* **2001**, *15*, 515—521.
(44) Clark, H. A.; Campagnola, P. J.; Wuskell, J. P.; Lewis, A.; Loew, L. M. *J. Am. Chem. Soc.* **2000**, *122*, 10234—10235.
(45) Jiang, Y.; Wilson, P. T.; Downer, M.; White, C. W. *Trends Opt. Photonics* **2000**, 46.
(46) Johnson, R. C.; Hupp, J. T. *Spectrum* **2000**, *13*, 3.
(47) Baldelli, S.; Eppler, A. S.; Anderson, E.; Shen, Y. R.; Somorjai, G. A. *J. Chem. Phys.* **2000**, *113*, 5432.
(48) Lamprecht, B.; Leitner, A.; Aussenegg, F. R. *Appl. Phys. B* **1999**, *68*, 419—423.
(49) Mendoza, B. S.; Mochan, W. L.; Maytorena, J. A. *Phys. Rev. B* **1999**, *60*, 14334.
(50) Sandrock, M. L.; Pibel, C. D.; Geiger, F. M.; Foss, C. A. *J. Phys. Chem. B* **1999**, *103*, 2668—2673.
(51) Eisenthal, K. B. *Chem. Rev.* **1996**, *96*, 1343.
(52) Berkovic, G.; Efrima, S. *Langmuir* **1993**, *9*, 355.
(53) Heinz, T. F. i.; Ponath, H. E.; Stegeman, G. I. *Nonlinear surface electromagnetic phenomena*; Elsevier Science Pub. Co.: Amsterdam, 1991.
(54) Hunter, R. J. *Introduction to modern colloid science*, 1st ed.; Oxford University Press: Oxford, U.K., New York, 1993.
(55) Hiemenz, P. C.; Rajagopalan, R. *Principles of colloid and surface chemistry*, 3rd ed.; Marcel Dekker: New York, 1997.
(56) Giordinaine, J. A. *Phys. Rev. A* **1963**, *138*, 1559.
(57) Bloembergen, N. *Nonlinear Optics*; Wiley: New York, 1965.
(58) Clays, K.; Persoons, A. *Phys. Rev. Lett.* **1991**, *66*, 2980.
(59) Terhune, R. W.; Maker, P. D.; Savage, C. M. *Phys. Rev. Lett.* **1965**, *14*, 681.
(60) Song, Q.; Wan, C. Z.; Johnson, C. K. *J. Phys. Chem.* **1994**, *98*, 1999.
(61) Aktsipetrov, O. A.; Elyutin, P. V.; Nikulin, A. A.; Ostrovskaya, E. A. *Phys. Rev. B* **1995**, *51*, 17591.
(62) Wang, H.; Yan, E. C. Y.; Borguet, E.; Eisenthal, K. B. *Chem. Phys. Lett.* **1996**, *259*, 15.
(63) Wang, H. F.; Yan, E. C. Y.; Liu, Y.; Eisenthal, K. B. *J. Phys. Chem. B* **1998**, *102*, 4446.
(64) Srivastava, A.; Eisenthal, K. B. *Chem. Phys. Lett.* **1998**, *292*, 345.
(65) Chattoraj, D. K.; Birdi, K. S. *Adsorption and the Gibbs surface excess*; Plenum Press: New York, 1984.
(66) Ross, S.; Morrison, I. D. *Colloidal systems and interfaces*; Wiley: New York, 1988.
(67) Adamson, A. W.; Gast, A. P. *Physical chemistry of surfaces*, 6th ed.; Wiley: New York, 1997.
(68) Myers, D. *Surfaces, Interfaces and Colloids — Principles and Applications*; VCH Publishers: New York, 1990.

(69) Masel, R. I. *Principles of adsorption and reaction on solid surfaces*; Wiley: New York, 1996.
(70) Kipling, J. J. *Adsorption from solutions of nonelectrolytes*; Academic Press: New York, 1965.
(71) Giles, C. H.; Nakhwa, S. N. *J. Appl. Chem.* **1962**, *12*, 266.
(72) Giles, C. H.; D'Silva, A. P.; Trivedi, A. S. *Proc. Int. Symp.* **1970**, 317.
(73) Somasundaran, P.; Markovic, B.; Yu, X.; Krishnakumar, S. i. In *Handbook of surface and colloid chemistry*; Birdi, K. S., Ed.; CRC Press LLC: Boca Raton, FL, 2003.
(74) Parfitt, G. D.; Rochester, C. H. *Adsorption from solution at the solid/liquid interface*; Academic Press: London, New York, 1983.
(75) Rosen, M. J. *Surfactants and interfacial phenomena*; Wiley: New York, 1978.
(76) Wang, H. F.; Troxler, T.; Yeh, A. G.; Dai, H. L. *Langmuir* **2000**, *16*, 2475.
(77) Davies, J. T.; Rideal, E. K. *Interfacial Phenomena*, 2nd ed.; Academic Press: New York, 1963.
(78) Eckenrode, H. M.; Dai, H. L. *Langmuir* **2004**, *20*, 9202.
(79) Eckenrode, H. M.; Jen, S. H.; Han, J.; Yeh, A. G.; Dai, H. L. *J. Phys. Chem. B* **2005**, *109*, 4646.
(80) Kerker, M. *The scattering of light, and other electromagnetic radiation*; Academic Press: New York, 1969.
(81) Bohren, C. F.; Huffman, D. R. *Absorption and scattering of light by small particles*; Wiley: New York, 1983.
(82) Hulst, H. C. v. d. *Light scattering by small particles*; Dover Publications: New York, 1981.
(83) Yang, N.; Angerer, W. E.; Yodh, A. G. *Phys. Rev. Lett.* **2001**, *8710*, No. 103902.
(84) Dadap, J. I.; Shan, J.; Eisenthal, K. B.; Heinz, T. F. *Phys. Rev. Lett.* **1999**, *83*, 4045.
(85) Snow, J. B.; Qian, S. X.; Chang, R. K. *Opt. Lett.* **1985**, *10*, 37.
(86) Hill, S. C.; Chang, R. K. *Studies in classical and quantum nonlinear optics*; Nova Science Publishers: Commack, NY, 1995.
(87) Hartings, J. M.; Poon, A.; Pu, X. Y.; Chang, R. K.; Leslie, T. M. *Chem. Phys. Lett.* **1997**, *281*, 389.
(88) Freeman, R. G.; Hommer, M. B.; Grabar, K. C.; Jackson, M. A.; Natan, M. J. *J. Phys. Chem.* **1996**, *100*, 718.
(89) Link, S.; El-Sayed, M. A. *J. Phys. Chem. B* **1999**, *103*, 8410.
(90) McConnell, W. P.; Novak, J. P.; Brousseau, L. C.; Fuierer, R. R.; Tenent, R. C.; Feldheim, D. L. *J. Phys. Chem. B* **2000**, *104*, 8925.
(91) Reynolds, R. A.; Mirkin, C. A.; Letsinger, R. L. *J. Am. Chem. Soc.* **2000**, *122*, 3795.
(92) Hao, E. C.; Schatz, G. C.; Johnson, R. C.; Hupp, J. T. *J. Chem. Phys.* **2002**, *117*, 5963.
(93) Agarwal, G. S.; Jha, S. S. *Solid State Commun.* **1982**, *41*, 499.
(94) Hua, X. M.; Gersten, J. I. *Phys. Rev. B* **1986**, *33*, 3756.
(95) Ostling, D.; Stampfli, P.; Bennemann, K. H. *Z. Phys. D* **1993**, *28*, 169.
(96) Martorell, J.; Vilaseca, R.; Corbalan, R. *Phys. Rev. A* **1997**, *55*, 4520.
(97) Makeev, E. V.; Skipetrov, S. E. *Opt. Commun.* **2003**, *224*, 139.
(98) Mertz, J.; Moreaux, L. *Opt. Commun.* **2001**, *196*, 325.
(99) Brudny, V. L.; Mendoza, B. S.; Mochan, W. L. *Phys. Rev. B* **2000**, *62*, 11152.
(100) Vance, F. W.; Lemon, B. I.; Hupp, J. T. *J. Phys. Chem. B* **1998**, *102*, 10091.
(101) Abid, J. P.; Nappa, J.; Girault, H. H.; Brevet, P. F. *J. Chem. Phys.* **2004**, *121*, 12577.
(102) Chen, C. K.; Heinz, T. F.; Ricard, D.; Shen, Y. R. *Phys. Rev. B* **1983**, *27*, 1965.
(103) Lambert, A. G.; Neivandt, D. J.; Briggs, A. M.; Usadi, E. W.; Davies, P. B. *J. Phys. Chem. B* **2002**, *106*, 10693.
(104) Michaels, A. M.; Nirmal, M.; Brus, L. E. *J. Am. Chem. Soc.* **1999**, *121*, 9932.
(105) Spiro, T. G.; Stigliani, W. M. *Chemistry of the environment*; Prentice Hall: Upper Saddle River, NJ, 1996.
(106) Schwarzenbach, R. P.; Gschwend, P. M.; Imboden, D. M. *Environmental organic chemistry*; Wiley: New York, 1993.
(107) Sposito, G. *The surface chemistry of soils*; Oxford University Press: New York, 1984.
(108) Bergna, H. E.; American Chemical Society. Division of Colloid and Surface Chemistry.; American Chemical Society. Meeting *The Colloid chemistry of silica: developed from a symposium sponsored by the Division of Colloid and Surface Chemistry, at the 200th National Meeting of the American Chemical Society, Washington, DC, August 26−31, 1990*; American Chemical Society: Washington, DC, 1994.
(109) Vance, F. W.; Lemon, B. I.; Ekhoff, J. A.; Hupp, J. T. *J. Phys. Chem. B* **1998**, *102*, 1845.
(110) Zhao, X. L.; Ong, S. W.; Eisenthal, K. B. *Chem. Phys. Lett.* **1993**, *202*, 513.
(111) Ong, S. W.; Zhao, X. L.; Eisenthal, K. B. *Chem. Phys. Lett.* **1992**, *191*, 327.
(112) Zhao, X. L.; Ong, S. W.; Wang, H. F.; Eisenthal, K. B. *Chem. Phys. Lett.* **1993**, *214*, 203.
(113) Zhao, X. L.; Subrahmanyan, S.; Eisenthal, K. B. *Chem. Phys. Lett.* **1990**, *171*, 558.
(114) Castro, A.; Bhattacharyya, K.; Eisenthal, K. B. *J. Chem. Phys.* **1991**, *95*, 1310.
(115) Abuin, E. B.; Lissi, E. A.; Nunez, R.; Olea, A. *Langmuir* **1989**, *5*, 753.
(116) Hobson, R. A.; Grieser, F.; Healy, T. W. *J. Phys. Chem.* **1994**, *98*, 274.
(117) Malyarenko, V. V.; Kuprienko, P. I. *Colloid J.* **1995**, *57*, 198.
(118) Takeoka, S.; Ohgushi, T.; Terase, K.; Ohmori, T.; Tsuchida, E. *Langmuir* **1996**, *12*, 1755.
(119) Larson, I.; Drummond, C. J.; Chan, D. Y. C.; Grieser, F. *J. Am. Chem. Soc.* **1993**, *115*, 11885.
(120) Hayes, K. F.; Redden, G.; Ela, W.; Leckie, J. O. *J. Colloid Interface Sci.* **1991**, *142*, 448.
(121) Stumm, W.; Huang, C. P.; Jenkins, S. R. *Croat. Chem. Acta* **1970**, *42*, 223.
(122) Westall, J. In *Geochemical Processes at Mineral Surfaces*; Davis, J. A., Hayes, K. F., Eds.; ACS symposium series 323; American Chemical Society: Washington, DC, 1986.
(123) Westall, J.; Hohl, H. *Adv. Colloid Interface Sci.* **1980**, *12*, 265.
(124) Davies, J. T. *Proc. R. Soc.* **1951**, *A208*, 224.
(125) McLaughlin, S. *Annu. Rev. Biophys. Biophys. Chem.* **1989**, *18*, 113.
(126) Yan, E. C. Y.; Liu, Y.; Eisenthal, K. B. *J. Phys. Chem. B* **1998**, *102*, 6331.
(127) Lyklema, J.; Overbeek, J. *J. Colloid Sci.* **1961**, *16*, 501.
(128) Abendroth, R. P. *J. Colloid Interface Sci.* **1970**, *34*, 591.
(129) Ahmed, S. M. *Can. J. Chem.* **1966**, *44*, 1663.
(130) Sposito, G. *The chemistry of soils*; Oxford University Press: New York, 1989.
(131) Olphen, H. v. *An introduction to clay colloid chemistry, for clay technologists, geologists, and soil scientists*; Interscience Publishers: New York, 1963.
(132) Lahav, N.; White, D.; Chang, S. *Science* **1978**, *201*, 67.
(133) Bernal, J. D. *Proc. Phys. Soc. B* **1949**, *62*, 597.
(134) Yan, E. C. Y.; Eisenthal, K. B. *J. Phys. Chem. B* **1999**, *103*, 6056.
(135) Fujishima, A.; Honda, K. *Nature* **1972**, *238*, 37.
(136) Ghosh, A. K.; Maruska, H. P. *J. Electrochem. Soc.* **1977**, *124*, 1516.
(137) Mills, A.; Davies, R. H.; Worsley, D. *Chem. Soc. Rev.* **1993**, *22*, 417.
(138) Vlachopoulos, N.; Liska, P.; Augustynski, J.; Gratzel, M. *J. Am. Chem. Soc.* **1988**, *110*, 1216.
(139) Gopidas, K. R.; Kamat, P. V. *J. Phys. Chem.* **1989**, *93*, 6428.
(140) Moser, J.; Gratzel, M. *J. Am. Chem. Soc.* **1984**, *106*, 6557.
(141) Boschloo, G. K.; Goossens, A.; Schoonman, J. *J. Electrochem. Soc.* **1997**, *144*, 1311.
(142) Oregan, B.; Gratzel, M. *Nature* **1991**, *353*, 737.
(143) Kamat, P. V.; Fox, M. A. *Chem. Phys. Lett.* **1983**, *102*, 379.
(144) Ellingson, R. J.; Asbury, J. B.; Ferrere, S.; Ghosh, H. N.; Sprague, J. R.; Lian, T. Q.; Nozik, A. J. *J. Phys. Chem. B* **1998**, *102*, 6455.
(145) Kurshev, V.; Kevan, L. *Langmuir* **1997**, *13*, 225.
(146) Moser, J.; Punchihewa, S.; Infelta, P. P.; Gratzel, M. *Langmuir* **1991**, *7*, 3012.
(147) Rodriguez, R.; Blesa, M. A.; Regazzoni, A. E. *J. Colloid Interface Sci.* **1996**, *177*, 122.
(148) Liu, Y.; Dadap, J. I.; Zimdars, D.; Eisenthal, K. B. *J. Phys. Chem. B* **1999**, *103*, 2480.
(149) Gennis, R. B. *Biomembranes: molecular structure and function*; Springer-Verlag: New York, 1989.
(150) Lasic, D. D. *Liposomes: from physics to applications*; Elsevier: Amsterdam; New York, 1993.
(151) Philippot, J. R.; Schuber, F. *Liposomes as tools in basic research and industry*; CRC Press: Boca Raton, FL, 1995.
(152) Liu, Y.; Yan, E. C. Y.; Eisenthal, K. B. *Biophys. J.* **2001**, *80*, 1004.
(153) Liu, Y.; Yan, C. Y.; Zhao, X. L.; Eisenthal, K. B. *Langmuir* **2001**, *17*, 2063.
(154) Yan, E. C. Y.; Eisenthal, K. B. *Biophys. J.* **2000**, *79*, 898.
(155) Shang, X. M.; Liu, Y.; Yan, E.; Eisenthal, K. B. *J. Phys. Chem. B* **2001**, *105*, 12816.
(156) Liu, J.; Shang, X.; Pompano, R.; Eisenthal, K. B. *Faraday Discuss.* **2005**, *129*, 291.
(157) Gregoriadis, G. *Liposomes as drug carriers: recent trends and progress*; Wiley: Chichester, U.K., New York, 1988.
(158) Lasic, D. D.; Papahadjopoulos, D. *Science* **1995**, *267*, 1275.
(159) Buster, D. C.; Hinton, J. F.; Millett, F. S.; Shungu, D. C. *Biophys. J.* **1988**, *53*, 145.
(160) Xiang, T. X.; Anderson, B. D. *Biophys. J.* **1997**, *72*, 223.
(161) Cafiso, D. S. *Methods Enzymol.* **1989**, *172*, 331.
(162) Cafiso, D. S.; Hubbell, W. L. *Biophys. J.* **1983**, *44*, 49.
(163) Wallach, D. F. H.; Winzler, R. J. *Evolving strategies and tactics in membrane research*; Springer-Verlag: New York, 1974.

(164) Eidelman, O.; Cabantchik, Z. I. *Biochim. Biophys. Acta* **1989**, *988*, 319.
(165) Moreaux, L.; Sandre, O.; Charpak, S.; Blanchard-Desce, M.; Mertz, J. *Biophys. J.* **2001**, *80*, 1568.
(166) Robertson, R. N. *The Lively membranes*; Cambridge University Press: Cambridge, U.K., New York, 1983.
(167) Yeagle, P. *The membranes of cells*, 2nd ed.; Academic Press: San Diego, CA, 1993.
(168) Mukherjee, S.; Chattopadhyay, A. *Biochemistry* **1996**, *35*, 1311.
(169) Robinson, A. J.; Richards, W. G.; Thomas, P. J.; Hann, M. M. *Biophys. J.* **1995**, *68*, 164.
(170) Papahadjopoulos, D.; Nir, S.; Ohki, S. *Biochim. Biophys. Acta* **1972**, *266*, 561.
(171) Demel, R. A.; Vandeene, L.; Bruckdor, K. *Biochim. Biophys. Acta* **1972**, *255*, 311.
(172) Szabo, G. *Nature* **1974**, *252*, 47.
(173) Martial, S.; Ripoche, P. *Anal. Biochem.* **1991**, *197*, 296.
(174) Carruthers, A.; Melchior, D. L. *Biochemistry* **1983**, *22*, 5797.
(175) Bittman, R.; Clejan, S.; Jain, M. K.; Deroo, P. W.; Rosenthal, A. F. *Biochemistry* **1981**, *20*, 2790.
(176) Xiang, T. X.; Anderson, B. D. *J. Membr. Biol.* **1995**, *148*, 157.
(177) Wehrli, S.; Ramirez, C.; Kraus, J. L.; Castaing, M. *Biochim. Biophys. Acta* **1992**, *1107*, 319.
(178) Shinitzky, M. *Physiology of membrane fluidity*; CRC Press: Boca Raton, FL, 1984.
(179) Marsh, D. *CRC handbook of lipid bilayers*; CRC Press: Boca Raton, FL, 1990.
(180) Lauger, P.; Stark, G. *Biochim. Biophys. Acta* **1970**, *211*, 458.
(181) Lauger, P.; Benz, R.; Stark, G.; Bamberg, E.; Jordan, P. C.; Fahr, A.; Brock, W. *Q. Rev. Biophys.* **1981**, *14*, 513.

CR0403685